Loss and Gain Measurements of Tensile-Strained Quantum Well Diode Lasers for Plasmonic Devices at Telecom Wavelengths

Daniele Costantini, Adel Bousseksou, Mickaël Fevrier, Béatrice Dagens, and Raffaele Colombelli

***Abstract*— We performed an experimental study of tensile strain quantum wells for diode lasers operating at telecom wavelengths and in transverse magnetic polarization. The optical losses of ridge waveguide resonators are measured with passive and active techniques. The results are consistent with the theory and provide a useful material parameter database for this kind of devices. With the aim of implementing active plasmonic devices we studied the effect of the proximity of the metal top contact to the laser active region.**

***Index Terms*— Integrated optoelectronics, optical losses, quantum well lasers.**

I. Introduction

SURFACE-PLASMON polaritons (SPP) are electromagnetic modes which propagate along metal-dielectric interfaces and are characterized by a strong perpendicular confinement. Recent interest in SPPs stems from their confinement properties and their ability to *follow* the surface material shape. It is possible in fact to simply guide and focus light using properly patterned metallic waveguides. Plasmonics hence provides new tools to control light propagation at the micro- and nano-scale [1]. A crucial step in the development of integrated plasmonic components is the realization of active plasmonic devices. Currently many efforts are devoted to the exploration of plasmon guiding and nanofocussing. Furthermore, several passive plasmonic components such as couplers, routers and filters have been successfully demonstrated and developed [2]. Until now however, SPPs are in most cases generated with an external laser source. In this scenario, integrated plasmon generation and/or amplification by electrical injection would constitute an essential step.

Recently we have demonstrated an integrated end-fire coupling approach for SPP generation by electrical injection in the mid-infrared (mid-IR) range of the electromagnetic spectrum, using a standard quantum cascade laser (QCL) as active source [3]. The same solution was also previously developed at telecom wavelengths [4], using a transverse magnetic (TM) polarized diode laser as source.

Manuscript received August 22, 2011; revised November 8, 2011; accepted November 22, 2011. Date of current version December 20, 2011. This work was supported in part by the French National Research Agency under Grant ANR-09-NANO-020 "Gospel".

The authors are with the Institut d'Electronique Fondamentale, University of Paris-Sud, Orsay 91405, France (e-mail: daniele.costantini@u-psud.fr; adel.bousseksou@u-psud.fr; mickael.fevrier@u-psud.fr; beatrice.dagens@u-psud.fr; raffaele.colombelli@u-psud.fr).

Color versions of one or more of the figures in this paper are available online at http://ieeexplore.ieee.org.

Digital Object Identifier 10.1109/JQE.2011.2178818

An alternative approach to the end-fire coupling is proposed in Ref. [5]. In this configuration, the top cladding dielectric waveguide layer is replaced by a patterned metallic layer which is located directly on top of the laser active region [6]. Metallic grating couplers - monolithically integrated in the device - are then employed to couple the laser mode to the passive metal-air plasmonic guide on the top device surface. This waveguide configuration enhances the coupling efficiency of surface plasmons waves into the passive waveguide, since the maximum of the laser mode profile is located in close proximity of the top metal-semiconductor interface.

The latter architecture suits the development of devices for the electrical generation of SPPs at telecom wavelengths. This goal requires a careful study: the metallic ohmic losses increase dramatically at short wavelengths, and the proximity of a metal layer to the laser active region can affect the laser performance, and even prevent lasing. We have recently developed designs to optimize the coupling between a laser source and a plasmonic waveguide in the telecom wavelength range [7]. We have clarified the dependence of the coupling efficiency on the system parameters and suggested optimal design strategies. An experimental realization of such a device requires a semiconductor laser operating at telecom wavelengths, with transverse magnetic (TM) polarization [8], and featuring a thin top-cladding layer.

In this paper we investigate the effect of the proximity of a metallic layer/contact to the active region of a TM-polarized tensile-strained diode laser [8]. In particular, we experimentally analyze the optical loss and the differential gain achievable. We have characterized two structures with identical active region (AR) cores, but featuring waveguides with different cladding thicknesses: a traditional waveguide - with thick dielectric claddings - and a thin cladding one, which allows us to place the metallic top contact in proximity of the active region. This is the suitable structure for plasmonic applications. We determine the optical losses using direct transmission measurements, and we obtain the differential optical gain (which we define in this paper as $\delta g/\delta J$, i.e. with respect to the injected current density) on the same devices with the Hakki-Paoli technique.

This analysis lays the foundation for the realization of active plasmonic devices in the telecom frequency range, where the so-called *thin cladding* structures (see next paragraph) will be employed as gain medium. We aim here at demonstrating the practical viability of this approach, and at benchmarking

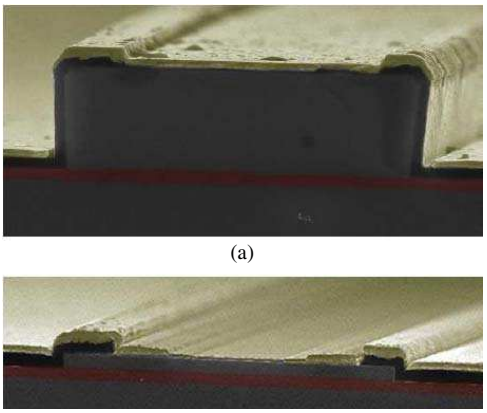

(a) (b)

Fig. 1. SEM images of the cleaved facets of (a) *thick cladding* and (b) *thin cladding* laser. The images are colorized (online version only) to highlight the different layer yellow is gold, green is the SiO_2 insulating layer, red is the active laser core.

laser performances, losses and achievable gain in view of implementing the devices proposed in Ref. [7].

The paper is organized as follows. Section II provides the description of the two investigated laser structures and the device processing. Section III contains the measurement of the optical waveguide losses *via* passive measurements. The gain measurements with Hakki-Paoli techniques on lasing devices are reported in section IV.

II. Structures Description and Device Processing

The TM polarized light is necessary in a planar coupling since the SPP electric field is perpendicular to the interface between the metal (gold) and the dielectric (air). QCLs naturally operate in TM polarization while diode lasers in the near-IR operate mostly in transverse electric (TE) polarization. A judicious source choice is therefore necessary. Our choice fell on diode lasers made of AlGaInAs tensile strained quantum wells, which represent the state-of-the-art TM source in the telecom wavelength range [8]. Compared to the quantum wells (QW) structures without tensile-strain, these structures have better performances, as a lower threshold current, and especially the TM field mode gain is significantly enhanced [9].

We have employed an optimized active region (AR) which contains 9 tensile strained semiconductor QWs. The growth was performed with metalorganic vapor phase epitaxy (MOVPE), as detailed in Ref. [8]. The detail layer-by-layer description of the two studied structures is reported in Table I(a). Our strategy is to analyze two structures with the same AR, but different top claddings layers, thick and thin, respectively detailed in Table I(b) and I(c). Claddings are grown by molecular beam epitaxy (MBE).

Both structures were fabricated into ridge waveguide resonators. The semiconductor claddings are etched until the stop layer above the AR. A 300-nm-thick Si_xN_y insulating layer is deposited by plasma-enhanced chemical vapor deposition (PECVD) and opened with reactive ion etching (RIE) on the top device surface. Ti/Au layers 3/200-nm-thick are e-beam evaporated to provide the electrical contact and - after polishing and back-contact deposition - the samples are cleaved and

TABLE I

(A) Detailed Structure of the Quantum-Well Based Laser Active Region. (B) Waveguide Details of the Thick Cladding Laser Structure. (C) Waveguide Details of the Thin Cladding Laser Structure

(A)	Type	Compostion	Strain	Thickness (nm)	♯ layers
	spacer	InP		50	1
	SCH-sup	GaInAsP		15	1
	Barrier	AlGaInAs	0.69%	19.6	9
	Well	AlGaInAs	−1.70%	9.5	9
	Barrier	AlGaInAs	0.69%	19.6	1
(B)	*Thick cladding*	Thickness (nm)		Doping (atm/cm^3)	
	InGaAs	300		3.00E+19	
	InP	2000		1.40E+18	
	InP	450		7.00E+17	
	InP	50		n.i.d	
(C)	*Thin cladding*	Thickness (nm)		Doping (atm/cm^3)	
	InGaAs	15		3.00E+19	
	InGaAsP	60		2.00E+19	
	InP	295		1.40E+18	

In-soldered onto copper blocks for characterizations. The laser ridges are typically 9-μm-wide, while their length L ranges from 350 μm to 4 mm. SEM images of the cleaved facets of two typical devices are shown in Fig. 1(a) (*thick cladding*) and Fig. 1(b) (*thin cladding*). A few devices featuring an *air confinement* waveguide were fabricated from the *thin cladding* structure [10]. In this case only narrow (1 μm-wide) lateral electrical contacts are present on the ridge top, leaving a 4 μm-wide central top region not covered by metallization layers.

III. Passive Measurements

Passive transmission measurements aim at quantifying the optical waveguide losses of our devices and they have been performed with no current injected in the laser. Linearly polarized light from a tunable laser is injected in the ridge resonator using a polarization-maintaining optical fiber, whose end is tapered and equipped with a micro lens. The transmitted signal is collected from the opposite facet with a microscope objective and focused onto a power-meter. A second polarizer is placed between the objective and the power-meter. It allows one to select the same polarization as the input signal, hence avoiding unwanted contributions from reflections and diffractions.

Preliminary transmission measurements were performed on a broad wavelength range (1.27 μm $< \lambda <$ 1.35 μm) to determine the polarization-dependent energy gap of the tensile-strained QWs. In order to minimize the background signal (due to multiple-reflections of the input signal) we measured 4-mm-long resonators. These long cavities can be measured only if the optical mode suffers weak losses. This corresponds to the case of *thick cladding* waveguides, where the top metallic contact is far from the AR. Fig. 2 shows the polarization dependency of the transmission signal at wavelengths close

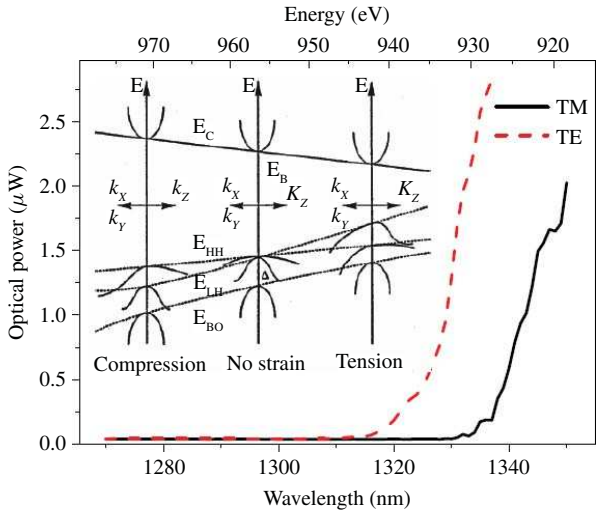

Fig. 2. Transmission curves for TE (red dashed curve) and TM (black solid curve) polarization in a *thick cladding* device of 4 mm length. The edge shift between the two polarizations transmission confirms that the energy gap for TM is lower than for TE polarization. The inset shows a scheme [19] of the effect of strain on the electronic band structure. Note that in the tensile strain case the energy gap between conduction and light-hole band (E_{LH}) is lower than any other gap.

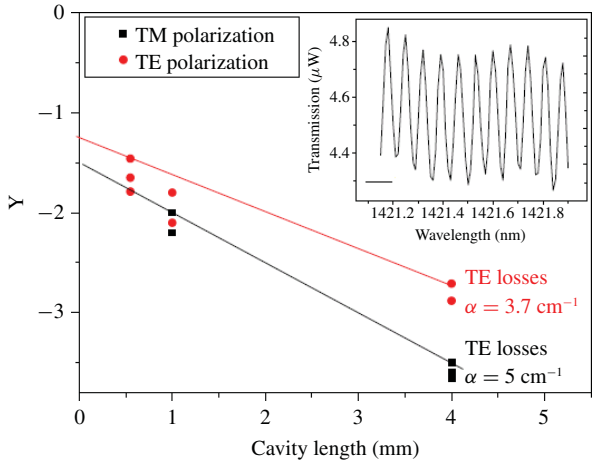

Fig. 3. Loss measurements on different cavity lengths (*thick cladding*) allows one to extrapolate the losses of the Fabry-Perot cavity. The lines slopes correspond to the cavity loss. Inset: Typical transmission measurement in a short wavelength range around 1420 nm.

to the energy gap. The absorption edge for TM polarization appears at lower energy than for TE polarization. These preliminary measurements attest that tensile strained QWs exhibit - as expected - a smaller energy gap for TM than for TE polarization [9].

In order to collect a stable transmission signal for both TE and TM polarizations, we performed the measurements in a wavelength range of about two nanometers around $\lambda =$ 1420 nm. This wavelength range is below the energy gap of the QWs. Inter-band absorption is absent, and we assume that the *transmission* losses at $\lambda =$ 1420 nm are similar to the *waveguide* losses at the shorter laser emission wavelength. An example of a high-resolution transmission scan is shown in the inset of Fig. 3. The free spectral range depends on the length of the laser cavity and is given by:

$$\Delta\lambda = \frac{\lambda^2}{2n_{eff}L} \tag{1}$$

where λ is the wavelength, n_{eff} the mode group index and L the cavity length. The oscillations in the transmitted signal are due to interferences in the Fabry-Perot cavity. The transmission contrast, defined as the ratio between the minimum ($P_{\min}$) and the maximum ($P_{\max}$) of the transmitted power, allows one to measure waveguide losses [11]. Using the following equation:

$$Y = \ln\left(\frac{1-\sqrt{P_{\min}/P_{\max}}}{1+\sqrt{P_{\min}/P_{\max}}}\right) = \ln(R) - \alpha_W^{TE/TM}L \tag{2}$$

where R is the mirror reflectivity. The Y parameter is extracted from the measured transmission contrast and it can be linked to the waveguide losses α_W, both for TE and TM polarization. Transmission measurements on different cavity lengths yield, *via* a simple linear fit, the waveguide loss and also the reflectivity coefficient R.

Fig. 3 shows the Y parameter as a function of cavity lengths and polarization for *thick cladding* devices. We have measured at least two different devices for every length. The linear fit yields the waveguide losses, which are $\alpha_W^{TE} = 3.7$ cm^{-1} and $\alpha_W^{TM} = 5$ cm^{-1}. The facet reflectivity is inferred from the linear fit and it is lower for the TM than for the TE mode. This trend is in reasonable agreement with results in the literature [12].

The experimentally measured α_W on the *thick cladding* devices allows us to finely adjust the material parameters used in the finite element numerical simulations [13] and to obtain a reliable tool to predict the optical losses in such heterostructures. We have performed the two dimensional simulation of the fundamental guided mode in our structure at a wavelength of 1420 nm. Every layer is characterized by a complex index of refraction where the imaginary part is linked to the material optical losses, as follows.

The absorption losses for the n-doped InP buffer are estimated using a Drude-Lorentz model. The losses for the p-doped layers are estimated *via* experimental measurements reported in Ref. [14], while the absorption coefficient in the thin InGaAs contact layer are taken from Ref. [15]. Finally, the index for gold $n_{gold} = 0.48 - i \times 9$ (at $\lambda =$ 1420 nm) is taken from [16].

In the *thick cladding* structures the electric field intensity at the top metal-semiconductor interface is negligible hence the losses are exclusively determined by absorption in the semiconductor layers. In order to reproduce the experimental data, we find that the absorption coefficient in the InP p-doped layers needs to be increased 2.5 times with respect to the values found in the literature [14]. These material parameters will therefore be used in the rest of the paper to perform the numerical simulations.

A summary of the theoretical and experimental waveguide losses (at $\lambda =$ 1420 nm) is reported in Table II. For TE-polarization, we obtain a good agreement between theory and experiment, for both *thin cladding* and *air-confinement* devices. However, in TM polarization α_W in *thin-cladding* devices are very sensitive to the top metal layer, hence their

TABLE II

EXPERIMENTAL AND CALCULATED OPTICAL VALUES AT A WAVELENGTH OF 1420 nm EXPRESSED IN cm^{-1}. IN TWO CASES IT WAS NOT POSSIBLE TO MEASURE THE TM LOSSES DUE TO THE EXTREMELY HIGH ABSORPTION VALUES

Waveguide cavity	Experimental losses		Simulation losses	
	TE	TM	TE	TM
Thi k cladding	3.7	5	3.7	5
Thin cladding	13	×	15.7	136.2
Air confinement on *thin cladding*	18	×	17.7	100.8

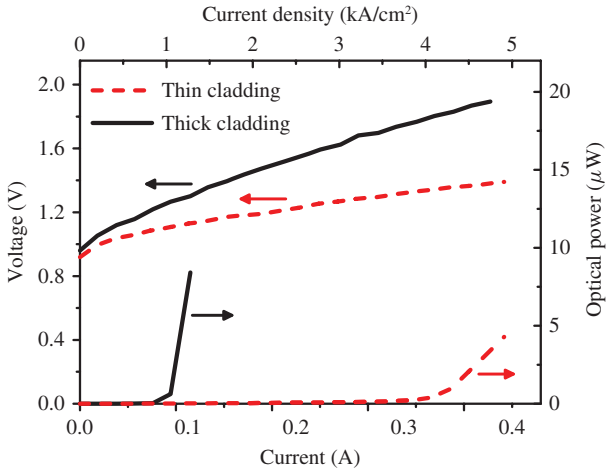

Fig. 4. Typical current- voltage (black-solid curve) and light-current (red-dashed curve) laser characterizations. The devices are 1000 × 9 μm^2 and they are measured at room temperature with 200-ns-wide pulses at a frequency of 100 kHz (DC = 2%).

losses considerably increase, up to more than 100 cm^{-1} (Table II, right column). This level of attenuation is incompatible with a passive loss measurement technique. This problem will be circumvented in the following section.

IV. ACTIVE MEASUREMENTS

Active measurements are performed upon electrical pumping of the devices, in pulsed or in continuous wave (CW) regime. The device output is collected using a cleaved multimode optical fiber which is either coupled to a high sensitivity power-meter (for light-current characterizations) or to an optical spectrum analyzer. In Fig. 4 we show typical light-current-voltage (LIV) characteristics of *thick-* and *thin-cladding* devices. (*Note:* the measured output powers are not representative of the total device output since we collect the signal with cleaved fibers in order to feed an optical spectrum analyzer). The measurements are performed at room-temperature, in pulsed regime with a 2% duty cycle (DC). Both devices reach laser threshold, even the *thin-cladding* devices which exhibit extremely large α_W. This is a promising result in view of developing fully plasmonic lasers at λ =1.3 μm. Typical thresholds (J_{th}) for *thick-cladding* devices are 1 − 1.5 kA/cm^2, while the *thin-cladding* devices exhibit J_{th} between 2.8 and 4 kA/cm^2.

We have applied the Hakki-Paoli method to experimentally measure the AR modal gain as a function of the emission

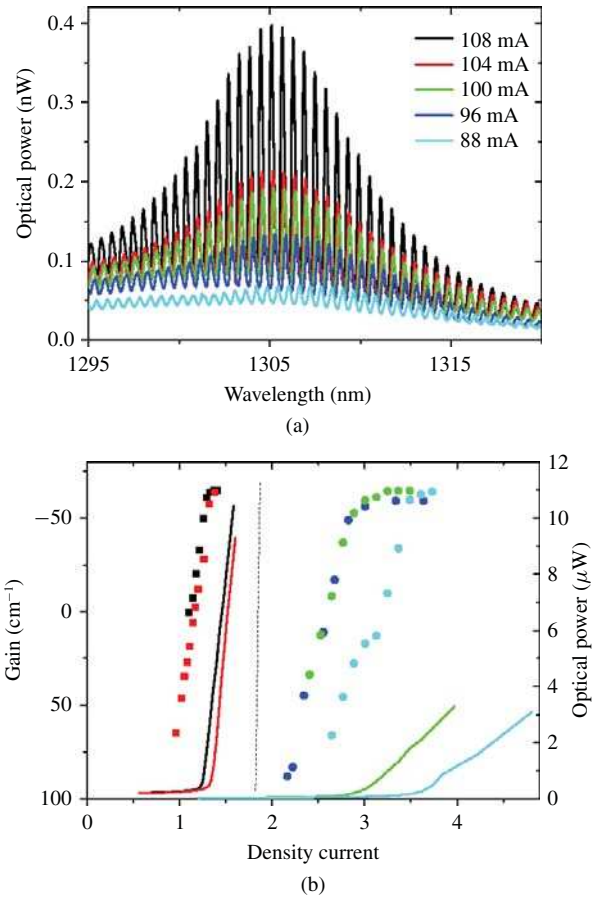

Fig. 5. (a) Spectra of a *thin cladding* device (350 μm long) at different current values below threshold. The spectra are collected in pulsed regime (frequency 1 MHz and pulse width of 100 ns, DC=10%). Every spectrum permits to infer a gain value with the Hakki-Paoli formula. (b) Laser output as function of injected current density (solid lines). The square and round dots represent the AR gain values for respectively *thick* and *thin* cladding as inferred from Hakki-Paoli measurements. All the laser cavities have a length of 350 μm.

wavelength [17]. (*Note:* the measurements have been performed at 10% DC). In particular, the gain can be determined as function of the injected current by collecting spectra below and above J_{th}. Fig. 5(a) shows typical spectra at different sub-threshold injected currents for the *thin cladding* device. The contrast between the interference fringes is defined as follows: $r(\lambda) = P_{min}(\lambda)/P_{max}(\lambda)$, where P_{min} and P_{max} are the minimum and maximum values of the Fabry-Perot spectrum. The modal gain can then be inferred using the following formula:

$$\Gamma g(\lambda) = \frac{1}{L}\ln\left(\frac{\sqrt{r(\lambda)}+1}{\sqrt{r(\lambda)}-1}\right) + \frac{1}{L}\ln(R). \qquad (3)$$

Where R is the facet power reflectivity and Ã is the guided mode overlap factor which we calculate at 0.55 for both *thick* and *thin* cladding waveguides. An important factor in a laser is the evolution of the optical gain with the injected current, whose slope represents the *differential gain* with respect to the current density ($\delta g/\delta J$). Fig. 5(b) shows the result of Hakki-Paoli measurements on *thick cladding* and *thin cladding* devices with cavity lengths of L=350 μm. The comparison with the LI curves shows that the gain increases almost linearly

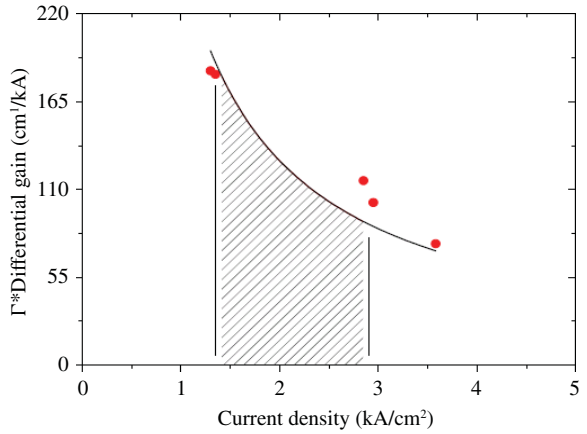

Fig. 6. Differential modal gain (with respect to the injected current density) 350-μm-long lasers as a function of the threshold density current. The values are obtained from Hakki-Paoli measurements. The general, expected trend is a decrease of the modal *differential gain* with the injected current density. The area of the shadowed surface corresponds to the gain needed to compensate the increased losses of *thin cladding* devices.

close to threshold, and it correctly clamps once lasing is achieved. The gain clamps at a value corresponding to the mirror losses (see eq. 3) which are determined by the cavity length L and the power reflectivity coefficient (R) of the facets.

A more careful analysis of Fig. 5(b) highlights that the *differential gain* decreases with the current density threshold, denoting a minor efficiency of the radiative recombination at high current densities. This again is in agreement with standard diode laser behavior.

Hakki-Paoli measurements were performed on several devices with different cladding types, cavity lengths and under pulsed or CW operation. *Thin cladding* devices only operate in pulsed mode, while *thick cladding* ones could be measured in both pulsed and CW regime. Operating in CW naturally reduces the *differential gain*, as well as operating longer-cavity devices, because of AR heating which decreases the efficiency of the radiative recombination. For this reason we concentrate on pulsed measurements in Fig. 6, which reports the results of gain measurements on several lasers with cavity length of 350 μm (which allows us to neglect heating effects). The *differential modal gain* (the mode overlap factor time the *differential gain*: $\Gamma \cdot \delta g/\delta J$) is plotted as function of the threshold current density.

At high injection currents the optical gain shows a saturation behavior and the *differential gain* decreases. The dependence of optical gain on the current density can be empirically fitted with the following logarithmic function [18]:

$$g = G_0 \ln\left(\eta_i \frac{J}{J_0}\right). \tag{4}$$

This empirical logarithmic gain-current density relation is a reasonable approximation essentially independent of recombination kinetics, which leads to a *differential gain* which is inversely proportional to the current density. We employ the following fitting function:

$$\frac{\delta g}{\delta J} = \frac{G_0}{J} \tag{5}$$

to fit the data on 350-μm-long lasers, which cover a broad span of J_{th}. We obtain $G_0 = 465 \pm 25$ cm^{-1}, in excellent agreement with the value found for a very similar AR (AlGaInAs\InP) by Van Parys and collaborators [19].

We can now estimate the losses of the thin-cladding lasers using the *differential gains* extracted from Hakki-Paoli measurements. By integrating the differential modal gain with respect to the current density the gain value of the laser can be calculated. The integration of $\Gamma \cdot \delta g/\delta J$ from typical thresholds of *thick-cladding* devices (J=1.3 kA/cm^2) to typical J_{th} of *thin-cladding* devices (about J=2.8 kA/cm^2) yields a gain difference of $\sim$200 cm^{-1}. This corresponds to the area of the shadowed surface in Fig. 6. This gain difference is of the same order of magnitude of the waveguide losses difference between thin and thick cladding devices that we have obtained in the previous section using passive, transmission measurements in combination with numerical simulations (Table II).

V. Conclusion

We fabricated ridge semiconductor lasers operating in TM polarization at wavelengths around 1.3 μm. We have studied the effect of the metal proximity to the laser active region. Passive measurements were performed injecting TE or TM polarized light in the ridge resonator. The optical losses were measured and found in agreement with finite element numerical simulations. Active measurements permitted an estimate of the active region *differential gain* using the Hakki-Paoli technique. The analysis of *differential gain* measurements is in agreement with literature results.

As expected, thinning the top cladding layer affects the laser performance. The threshold current density increases by a factor of $\sim$3 with respect to standard devices. Nevertheless, the thin cladding devices operate at room temperature, thus validating their use as sources to couple surface plasmons into passive waveguides [7]. The complete understanding of thin cladding structures is a preliminary step for the development of plasmonic devices using diode laser active regions. The next logical step will be the realization of a distributed feedback (DFB) laser with a top metallic grating. It will simultaneously provide loss reduction *via* metal patterning [6] and spectrally single mode emission, and it will represent the first building block for plasmonic generation by electrical injection at telecom wavelengths.

Acknowledgment

The authors would like to thank J. Decobert, F. Lelarge, J-L. Gentner, A. Accard, G. Duan (Alcatel/Thales III–V Laboratory, Paris, France) for the sample epitaxy and useful discussions. The device fabrication has been performed at the nano-center CTU-IEF-Minerve. We thank L. Vivien and D. Marris-Morini for help with the measurement setup.

References

[1] T. W. Ebbesen, C. Genet, and S. I. Bozhevolnyi, "Surface-plasmon circuitry," *Phys. Today*, vol. 61, no. 5, pp. 44–51, 2008.

[2] D. Gramotnev and S. I. Bozhevolnyi, "Plasmonics beyond the diffraction limit," *Nature Photon.*, vol. 4, pp. 83–91, Jan. 2010.

[3] J.-P. Tetienne, A. Bousseksou, D. Costantini, R. Colombelli, A. Babuty, I. Moldovan-Doyen, Y. De Wilde, C. Sirtori, G. Beaudoin, L. Largeau, O. Mauguin, and I. Sagnes, "Injection of midinfrared surface plasmon polaritons with an integrated device," *Appl. Phys. Lett.*, vol. 97, no. 21, pp. 211110-1–211110-3, Nov. 2010.
[4] C. S. Kim, I. Vurgaftman, R. A. Flynn, M. Kim, J. R. Lindle, W. W. Bewley, K. Bussmann, J. R. Meyer, and J. P. Long, "An integrated surface-plasmon source," *Opt. Exp.*, vol. 18, no. 10, pp. 10609–10615, 2010.
[5] A. Babuty, A. Bousseksou, J.-P. Tetienne, I. M. Doyen, C. Sirtori, G. Beaudoin, I. Sagnes, Y. De Wilde, and R. Colombelli, "Semiconductor surface plasmon sources," *Phys. Rev. Lett.*, vol. 104, no. 22, pp. 226806-1–226806-4, Jun. 2010.
[6] A. Bousseksou, Y. Chassagneux, J. R. Coudevylle, R. Colombelli, C. Sirtori, G. Patriarche, G. Beaudoin, and I. Sagnes, "Surface-plasmon distributed-feedback quantum cascade lasers operating pulsed, room temperature," *Appl. Phys. Lett.*, vol. 95, no. 9, pp. 091105-1–091105-3, Aug. 2009.
[7] J.-P. Tetienne, A. Bousseksou, D. Costantini, Y. De Wilde, and R. Colombelli, "Design of an integrated coupler for the electrical generation of surface plasmon polaritons," *Opt. Exp.*, vol. 19, no. 19, pp. 18155–18163, 2011
[8] J. Decobert, N. Lagay, C. Cuisin, B. Dagens, B. Thedrez, and F. Laruelle, "MOVPE growth of AlGaInAs/InP highly tensile-strained MQWs for 1.3 μm low-threshold lasers," *J. Cryst. Growth*, vol. 272, nos. 1–4, pp. 543–548, 2004.
[9] P. J. A. Thijs, L. F. Tiemeijer, J. J. M. Binsma, and T. van Dongen, "Progress in long-wavelength strained-layer InGaAs(P) quantum-well semiconductor lasers and amplifiers," *IEEE J. Quantum Electron.*, vol. 30, no. 2, pp. 477–499, Feb. 1994.
[10] V. Moreau, M. Bahriz1, R. Colombelli, R. Perahia, O. Painter, L. R. Wilson, and A. B. Krysa, "Demonstration of air-guided quantum cascade lasers without top claddings," *Opt. Exp.*, vol. 15, no. 22, pp. 14861–14869, 2007.
[11] T. Feuchter and C. Thirstrup, "High precision planar waveguide propagation loss measurement technique using a Fabry-Perot cavity," *IEEE Photon. Technol. Lett.*, vol. 6, no. 10, pp. 1244–1247, Oct. 1994.
[12] H. C. Casey and M. B. Panish, *Heterostructured Lasers, Part A*. New York: Academic, 1978, p. 80.
[13] *COMSOL: Multiphysics Finite Element Analysis Simulation Software* [Online]. Available: http://www.comsol.com/products/multiphysics/
[14] H. C. Casey and P. L. Carter, "Variation of intervalence band absorption with hole concentration in p-type InP," *Appl. Phys. Lett.*, vol. 44, no. 1, pp. 82–83, Jan. 1984.
[15] S. Adachi, *Physical Properties of III–V Semiconductor Compounds*. New York: Wiley, 1992.
[16] E. D. Palik, *Handbook of Optical Constants*. New York: Academic, 1998.
[17] B. W. Hakki and T. L. Paoli, "Gain spectra in GaAs double-heterostructure injection lasers," *J. Appl. Phys.*, vol. 46, no. 3, pp. 1299–1306, Mar. 1975.
[18] T. A. De Temple and C. M. Herzinger, "On the semiconductor laser logarithmic gain-current density relation," *IEEE J. Quantum Electron.*, vol. 29, no. 5, pp. 1246–1252, May 1993.
[19] W. Van Parys, "Optimization of an integrated optical isolator based on a semiconductor amplifier with a ferromagnetic metal contact," Ph.D. dissertation, Dept. INTEC, Ghent Univ., Ghent, Belgium, 2009.

Daniele Costantini was born in Meyrin in 1984. He received the B.S. degree in physics and the M.S. degree in solid state physics from the University of Pisa, Pisa, Italy, in 2006 and 2009, respectively. He is currently pursuing the Ph.D. degree with Institut d'Electronique Fondamentale, University of Paris-Sud, Orsay, France.

His current research interests include analysis of transport properties and photoconductive response of single InAs nanowires, semiconductor plasmonic devices, surface plasmon generation, and amplification.

Adel Bousseksou received the Ph.D. degree in physics from University Paris-Sud, Orsay, France, in 2007.

He joined the Laboratory of Photonics and Nanostructures, Marcoussis, France, where he developed electrically driven vertical cavity surface emitting lasers at telecom wavelengths. He joined Institut d'Electronique Fondamentale, University of Paris-Sud, as a Post-Doctoral Researcher. His current research interests include quantum cascade lasers employing plasmonic waveguides and the development of device concepts for coupling/generation of surface plasmons using semiconductor lasers.

Dr. Bousseksou is Maitre de Conferences with University Paris Sud since September 2010.

Mickaël Fevrier received the M.S. degree in optics and nanotechnology from the University of Technology of Troyes, Troyes, France, in 2008. He is currently pursuing the Ph.D. degree with Institut d'Electronique Fondamentale, University of Paris-Sud, Orsay, France.

His current research interests include plasmonics and silicon photonics.

Béatrice Dagens received the Masters degree in physics and chemistry from Ecole Supérieure de Physique et de Chimie Industrielles, Paris, France, the Ph.D. degree in optoelectronics from University Paul Sabatier, Toulouse, France, and the H.D.R (habilitation) degree from University Paris-Sud, Orsay, France, in 1992, 1995, and 2005, respectively.

She joined the Optical Component Research Department, Alcatel, Marcoussis, France, in 1996. She was first responsible for design, realization and the measurement of semiconductor optical amplifier based interferometers for all-optical and high bit rate wavelength conversion and regeneration. She has been a Senior Researcher with Institut d'Electronique Fondamentale, Orsay, since 2007. She has been co-responsible for Photonic Department since 2011. She has authored and co-authored more than 120 international publications, communications, and 15 patents. Her current research interests include advanced laser diodes emitting at 1.3 and 1.55 μm using new materials like quantum dots, dilute nitride based active layers, metallic ferromagnetic layers, photonics integrated circuits, magneto-optical, magneto-photonic, and plasmonic nanostructured waveguides for compact integrated photonic circuits.

Raffaele Colombelli received the Ph.D. degree in physics from Scuola Normale Superiore, Pisa, Italy, in 1999, for his work on the optical properties of ultra-thin layer insertions in semiconductor host materials.

He joined Bell Laboratories, Murray Hill, NJ, where he focused on long-wavelength quantum cascade lasers, and the application of photonic technology to unipolar devices. In 2003, he joined the National Center for Scientific Research, Institut d'Electronique Fondamentale, Orsay, France, where he is the Research Director. He is the co-author of more than 80 papers in peer reviewed international journals. His current research interests include development of terahertz semiconductor devices, applications of photonic crystal technology to quantum cascade lasers, and mid-/near-infrared plasmonics.